Responses to reviewer 1: discussion (`acp-2020-136`)

September 15, 2020

The authors would like to thank Alexei Korolev for taking the time to review the manuscript and for his constructive feedback. We hope the responses provided below help to clarify the issues addressed. The adjustments made to the manuscript resulting from the feedback are summarized at the end of each response.

Remark by the authors In the original "referee comment", the reviewer is not referring to the latest version of the manuscript, but to the pre-discussion version. The line numbers and equation numbers have been adapted in the following to reflect the discussion paper.

1 Comments

R1-Co1. Since it was not specified in the text, it appears that Eq. 16 assumes that the lifetime of all hydrometeors is the same. This assumption would work well for riming particles falling through a mixed phase environment. However, the condition $T_p = 0°C$ will be limited by the freezing time of drops and should be accounted for in Eq. 16. Since freezing time for large and small drops may be different by few orders of magnitude (e.g. Murray and List, 1972), the effect of small droplets on the supersaturated volume may be lower than shown in Fig. 6. The following results obtained in this work will also be affected. The effect of freezing time for the case of freezing drops requires clarification.

The results of this work should be considered as a best-case scenario for ice enhancement, i.e. how much ice enhancement is to be expected at very favorable conditions. We agree with the reviewer that the assumption of $T_p = 0°C$ is more suitable for riming ice than for freezing drops, and it will be stated more clearly in the revised manuscript that riming ice is the main mechanism considered in this work.

When freezing drops are considered, $T_p = 0°C$ is still a good approximation for the surface temperature in case of inward freezing (Johnson and Hallett, 1968), however, unlike in the case of riming ice, there is no mechanism which sustains the gap in surface to ambient temperature after the freezing time is exceeded. The temperature distribution (for a given meteor size) will therefore not be concentrated on a single value, and instead, the rate at which new unfrozen droplets are available, the rate at which fully frozen droplets deplete and the size population dynamics with history effects have to be taken into account. Qualitatively, ice enhancement will be lower than the estimation given in the present work when the freezing time is taken into consideration. Because the freezing time is correlated positively to the meteor size, this deviation is expected to be more significant at low cloud temperatures, since the size distribution shifts towards lower values the lower the cloud temperature is. Therefore, freezing drops are even less likely to generate significant amounts of secondary ice than riming ice particles.
Adjustments to the manuscript: A paragraph will be added to the manuscript to emphasize this point.

R1-Co2. The supersaturation calculation was considered for a particle free falling in still air, i.e. in a non- turbulent environment ($\epsilon = 0$). Could you speculate on a qualitative level, how $\epsilon > 0$ may affect your results? Would it increase or decrease the global ice

enhancement factor?

The study of Bagchi and Kottam (2008) is very helpful when the effect of ambient turbulence on the supersaturated volume and ice enhancement is discussed. The parameter range investigated in their work corresponds reasonably well to the scenario of a hydrometeor with a diameter of a few millimeter settling under atmospheric conditions, where the largest flow scales are expected to be $\mathcal{O}(100\text{m})$ and the smallest scales around $\mathcal{O}(1\text{mm})$ (Lehmann, Siebert, and Shaw, 2009).

We know from simple mixing parcel models (e.g. (Chouippe, Krayer, Uhlmann, Dušek, Kiselev, and Leisner, 2019, fig. 17) or (Prabhakaran, Kinney, Cantrell, Shaw, and Bodenschatz, 2020, fig. 4)) that the highest supersaturations occur in regions where the temperature of the mixture is roughly halfway between T_∞ and T_p, i.e. $\tilde{T} \approx 0.5$ with $\tilde{T}$ being the non-dimensionalized temperature as introduced in the manuscript. In (Bagchi and Kottam, 2008, fig. 17) it is demonstrated that the centerline temperature in the wake decays significantly faster if the background flow is turbulent, especially when $\tilde{T} \lessapprox 0.4$. Therefore it is to be expected that supersaturation decays faster in the wake than it does for a uniform inflow, and thus, the supersaturated volume as well as the ice enhancement are most likely smaller if the ambient is turbulent.

However, Bagchi and Kottam (2008) also investigated the the effect of turbulence on the heat and mass transfer coefficient. While the mean value of the Nusselt number remains mostly unaffected, strong fluctuations in its value can be observed. This presumably leads to a more intermittent behavior of the temperature and vapor fields. The role of intermittency on ice nucleation activity still needs to be investigated more thoroughly, especially when the distribution of aerosol particles is explicitly considered (a point which was suggested to be investigated as part of future work). If regions of strong supersaturation conincide with regions where AP are preferentially located, intermittency might promote ice nucleation as supersaturation and nucleation rate are non-linearly linked to the temperature/vapor fields.

Adjustments to the manuscript: A paragraph discussing the influence of turbulence will be added to the manuscript.

Note: This response is the same as the response to remark R2-Co2 raised by reviewer 2, due to the strong similarity of the remarks.

R1-Co3. What is the role of air pressure P on the results obtained in this paper (specifically Fig. 9)? Since particle fall speed, viscosity and thermal conductivity depend on P, it may have a noticeable effect on the mixing rate, supersaturated volume, amplitude of result supersaturation and the persistence of supersaturated regions. It is worth indicating what P was used in this study.

For the numerical simlations, no assumptions on the actual value of pressure have to be made since the incompressible Navier-Stokes equations are independent of the absolute value of pressure and the only imposed parameters in our framework are the particle Reynolds number, the Prandtl number and the Schmidt number, whose definitions are

$$Re = \frac{v_p D}{\nu},\ Pr = \frac{\nu}{D_T},\ Sc = \frac{\nu}{D_{n_v}}$$

where the dependency on the fluid density is approximately $\nu \sim \rho^{-1}$, $D_T \sim \rho^{-1}$ and $D_{n_v} \sim \rho^{-1}$ in the low density limit (see e.g. Bird, Stewart, and Lightfoot (2002)). Throughout this work, air is assumed to be an ideal gas and therefore

$$P \propto \rho T. \tag{1}$$

The only parameter affected by a variation in pressure is therefore the Reynolds number due to the modification in viscosity and fall speed of the hydrometeor. However, in the majority of the manuscript the dependency on the Reynolds number is neglected except for transitions in flow regimes. Therefore, the only relevant quantity within the framework of this work which is affected by the absolute value of pressure is the threshold diameter for regime transition (see response to R1-Co5 for the relationship). However, this quantity is already subject to various uncertainties such as the shape of the hydrometeor (affecting fall speed and flow regimes) and its density such that taking into account different pressure levels does not seem worthwhile. The supersaturated volume scaled by the hydrometeor volume is of similar order of magnitude for both regimes investigated. Therefore, a shift in threshold diameter for transition alone is unable to lead to a significant alteration of the global ice enhancement factor.

In this work, the density of ambient air was assumed to be $1\,\mathrm{kg\,m^{-3}}$ which approximately corresponds to the values of atomospheric pressure presented in table 1 in the temperature range investigated according to the ideal gas equation of state.

temperature [°C]	−40	−30	−20	−10	0
pressure [kPa]	669	698	727	755	783

Table 1: Ambient air pressure for different air temperatures investigated.

R1-Co4. An important element not discussed in this study is the conceptual consideration of how this SIP process is related to natural clouds and identification of environmental conditions when it becomes significant. There are a few statements regarding this matter scattered throughout the manuscript. However, it leaves the reader with an impression of incompleteness of this paper. For example, as discussed in section 2, the condition $T_p = 0°\mathrm{C}$ can be satisfied for riming ice particle or freezing drops. For the first case, the accretion of cloud droplets on the ice surface should reach the wet growth regime, i.e. when LWC reach the Ludlam limit. At $-30°\mathrm{C}$, for a free-falling hailstone, the Ludlam limit exceeds $5\mathrm{g\,m^{-3}}$ (the exact number needs to be checked). Such high LWC at $-30°\mathrm{C}$ does not seem to be feasible. Regarding the second case, there are very few reports on observations of precipitation size drops ($D > 100\mathrm{\mu m}$) at $-30°\mathrm{C}$. Therefore, this option also appears to be uncommon in clouds. In addition to the discussion on page 11 related to Fig. 9, it is worth expanding the discussion about the feasibility and significance of this SIP mechanism in temperatures warmer than $-30°\mathrm{C}$. Mentioning that convective clouds are the most likely candidates for this type of SIP to occur would be also relevant.

The reviewer is correct that wet-growth at low cloud temperatures only occurs if the LWC is sufficiently high, and we arrive at a similar estimation for the Ludlam limit when applying the empirical formula of García-García and List (1992),

$$W_{f,SLL} = -2 \cdot 10^{-4} \frac{\mathrm{kg}}{\mathrm{m^3\,°C}} T_\infty, \tag{2}$$

which results in $W_{f,SLL} = 6\mathrm{g\,m^{-3}}$ for $T_\infty = -30°\mathrm{C}$. Such high LWC and temperature gaps between the hydrometeors surface and the ambient exceed the range of values commonly observed in natural clouds, and merely served the purpose of demonstrating that exceptional/unrealistic conditions are required for this mechanism to be relevant. In accordance to the response given in R2-Ma1, we have decided to adjust the temperature range investigated and to focus on temperatures warmer than $-15°\mathrm{C}$. The discussion on fig. 9 will be rewritten accordingly. The revised versions of all affected figures may be found in section 2 of this document.

We will also add a paragraph discussing the required cloud conditions to the manuscript, where the relevance of high LWC is emphasized. We agree that convective clouds are the most likely candidates for the required conditions.

Adjustments to the manuscript: The temperature range investigated is adjusted. Revised versions of all affected figures can be found in section 2 of this document. The text in the manuscript will be adjusted accordingly. A paragraph discussing the required environmental conditions and possible cloud types in which they occur is added to the manuscript.

R1-Co5. Eq.10: What $D_{j,min}$ and $D_{j,max}$ were used in this study? It is worth indicating the in the text.

The diameter thresholds were determined from the critical Reynolds numbers of regime transition Re_c

using the following set of equations.

$$Re_{c,j} = D_{j,max}|v_p|/\nu$$
$$v_p = u_g\left(3C_d(Re_{c,j})/4\right)^{-1/2}$$
$$u_g = \sqrt{\left(\rho_p/\rho_f - 1\right)|g|D_{j,max}}$$

The drag coefficient is approximated using the empirical drag law of Schiller and Naumann (1933). The density of the hailstone is assumed to be 600kg m^{-3}, as has been stated in the main text, and the fluid density was set to 1kg m^{-3} (see also the response to R1-Co3 concerning this). Furthermore, the kinematic viscosity was set constant to $1 \cdot 10^{-5}$m^2 s^{-1} in the discussion paper, but has been revised to a value of $1.68 \cdot 10^{-5}$m^2 s^{-1} in the revised version of the manuscript, which corresponds approximately to the value at 750kPa air pressure and −10°C ambient temperature.

For Fig. 2 and Fig. 3 in the discussion paper, all four regimes are considered and the values of Re_c have been chosen in accordance to the values stated in section 3.1 of the discussion paper. The threshold diameters used in the discussion paper (D^{old}_{min}, D^{old}_{max}) and the revised manuscript (D^{new}_{min}, D^{new}_{max}) are summarized in table 2.

regime	D^{old}_{min}	D^{old}_{max}	D^{new}_{min}	D^{new}_{max}	Re_c
axisymmetric	0	0.77 mm	0	1.08 mm	212
steady oblique	0.77 mm	0.88 mm	1.08 mm	1.24 mm	273
oscillating oblique	0.88 mm	1.0 mm	1.24 mm	1.44 mm	360
chaotic	1.0 mm	∞	1.44 mm	∞	–

Table 2: Threshold diameters for regime transition used in the discussion paper (D^{old}_{min}, D^{old}_{max}) and the revised manuscript (D^{new}_{min}, D^{new}_{max}).

From section 3.2 onward, only the axisymmetric and chaotic regimes are considered and the following theshold diameter has been chosen for concreteness.

regime	D^{old}_{min}	D^{old}_{max}	D^{new}_{min}	D^{new}_{max}
axisymmetric	0	0.85 mm	0	1.26 mm
chaotic	0.85 mm	∞	1.26 mm	∞

Adjustments to the manuscript: The threshold diameters will be stated in the text.

R1-Co6. Definition of $\tilde{s}^*_i$ is worth introducing in the text prior to Fig.4.
We agree that either the caption should be rephrased or the concept $\tilde{s}_i$ should be introduced in the text before referring to the figure.

R1-Co7. Line 222: Should it be $\tilde{s}^*_i$?
In this case, we are not referring to a threshold (as we do for the supersaturated volume), but to the supersaturation field itself, i.e. $\tilde{s}_i = \tilde{s}_i(\mathbf{x}, t)$. The expression in line 222 may be rephrased as $s_i(\mathbf{x}, t) > s_{i,\infty}$.

R1-Co8. Eq.16. Definitions of τ and Ω should be provided in the text.
We thank the reviewer for bringing this to our attention. Indeed the definitions of τ and Ω are absent in the text and will be added in the revised version of the manuscript. τ denotes the time over which the flow is time-averaged and Ω denotes the simulation domain, i.e. in this case a volume integral is computed over the entire domain of observation.

R1-Co9. Line 227: "... as a function of the threshold". I guess you employed $\tilde{s}^*_i = 0.1$ threshold. This should be indicated in the text.
This appears to be a misunderstanding. Eq. (16) in the discussion paper is an expression which

computes the volume of fluid in the domain of observation which is supersaturated at a value higher than a given value (the threshold s_i^*), i.e. it answers the question "How much fluid volume exhibits a supersaturation of at least s_i^*?". In figure 6 of the discussion paper, the resulting volume is shown for varying thresholds, which are in the figure given as offsets from $s_{i,\infty}$. However, for reasons explained in the response to R2-Ma2, the supersaturated volume will be given as a function of s_i^* instead of $\tilde{s}_i^* = s_i^* - s_{i,\infty}$ in the revised version of the manuscript (see fig. 3 of this document).

R1-Co10. Lines 24 and 358: Field et al. 2016 should be 2017.
We thank the reviewer for pointing out this mistake, which will be corrected in the revised version of the manuscript.

2 Figures

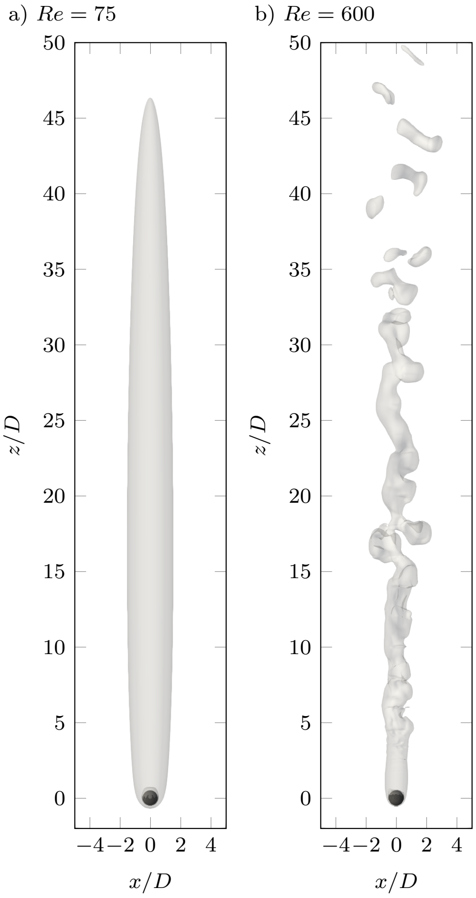

Figure 1: Isosurfaces of supersaturation in the wake at $T_\infty = -15$°C. The value of the isocontour is $\tilde{s}_i^* = 0.02$, i.e. two percentage points higher than the ambient supersaturation. Two different wake regimes are depicted, which correspond to two different hydrometeor sizes in our framework. (a) axisymmetric regime at $Re = 75$, (b) chaotic regime at $Re = 600$.

`Changelog: changed ambient temperature to` $T_\infty = -15$°C`; changed isocontour threshold to` $\tilde{s}_i^* = 0.02$`; adapted caption accordingly`

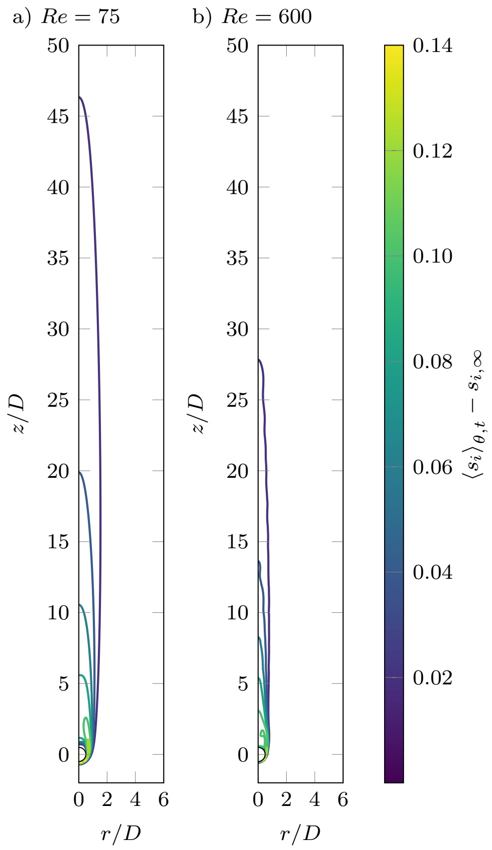

Figure 2: Contours of excess supersaturation in the wake, averaged over time and azimuthal direction at $T_\infty = -15$°C. (a) axisymmetric regime at $Re = 75$, (b) chaotic regime at $Re = 600$.
`Changelog: changed ambient temperature to` $T_\infty = -15$°C`; adapted caption accordingly`

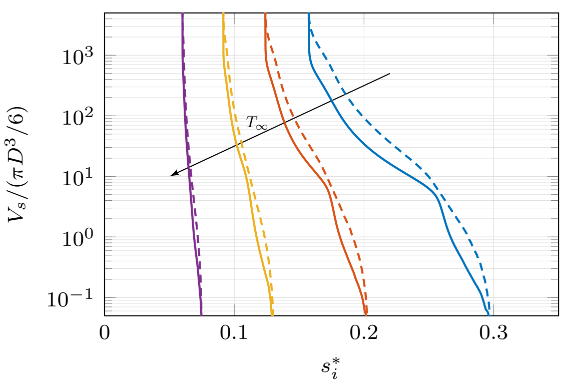

Figure 3: Volume of air where supersaturation w.r.t. ice exceeds a given threshold as a function of the threshold. The volume is normalized by the volume of the ice particle and four different ambient temperatures are shown: $T_\infty = -6$°C (——), $T_\infty = -9$°C (——), $T_\infty = -12$°C (——). $T_\infty = -15$°C (——). Solid lines correspond to $Re = 600$ (chaotic regime), while dashed lines show the data obtained for $Re = 75$ (axisymmetric regime).
`Changelog: changed ambient temperature range; added` T_∞ `indicator; adapted caption accordingly`

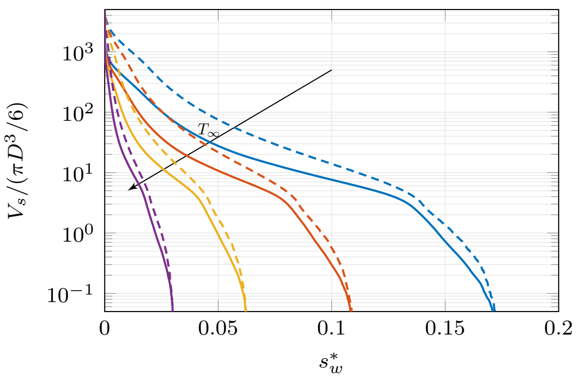

Figure 4: Volume of air where supersaturation w.r.t. liquid exceeds a given threshold as a function of the threshold. The volume is normalized by the volume of the ice particle and four different ambient temperatures are shown: $T_\infty = -6$°C (——), $T_\infty = -9$°C (——), $T_\infty = -12$°C (——). $T_\infty = -15$°C (——). Solid lines correspond to $Re = 600$ (chaotic regime), while dashed lines show the data obtained for $Re = 75$ (axisymmetric regime).

`Changelog: new figure`

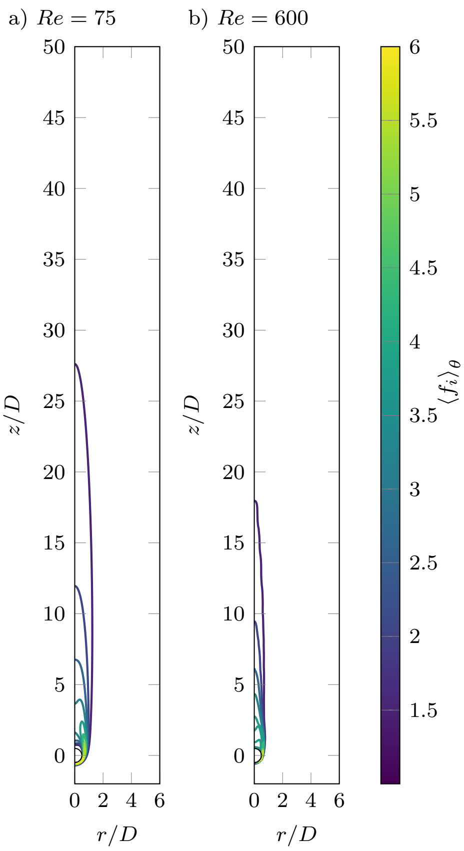

Figure 5: Contours of local ice enhancement factor in the wake, averaged over time and azimuthal direction at $T_\infty = -15$°C. (a) axisymmetric regime at $Re = 75$, (b) chaotic regime at $Re = 600$.

`Changelog: changed ambient temperature to` $T_\infty = -15$°C`; contour lines are now linearly spaced; ice enhancement computed according to deposition nucleation law provided by Meyers et al. (1992); adapted caption accordingly`

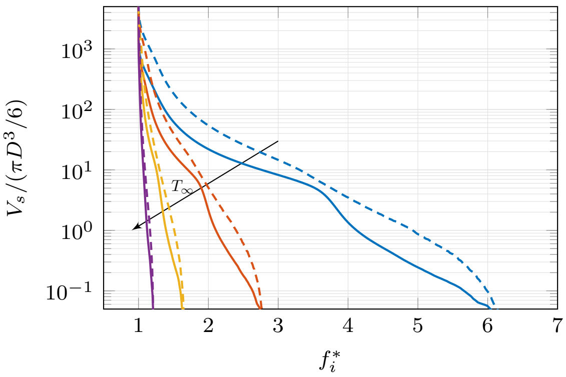

Figure 6: Volume of air with supersaturation above a given threshold as a function of the ice enhancement factor. The volume is normalized by the volume of the ice particle and four different temperatures are shown: $T_\infty = -6°\mathrm{C}$ (——), $T_\infty = -9°\mathrm{C}$ (——), $T_\infty = -12°\mathrm{C}$ (——). $T_\infty = -15°\mathrm{C}$ (——). Solid lines correspond to $Re = 600$ (chaotic regime), while dashed lines show the data obtained for $Re = 75$ (axisymmetric regime).

`Changelog: changed ambient temperature range; ice enhancement computed according to deposition nucleation law provided by Meyers et al. (1992); x-axis now linearly spaced; added` T_∞ `indicator; adapted caption accordingly`

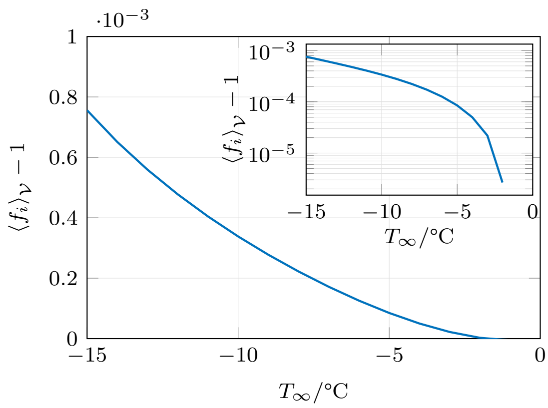

Figure 7: Global ice enhancement factor as a function of cloud temperature. The inset shows the same data, but in semi-logarithmic scale.

`Changelog: changed ambient temperature range; ice enhancement computed according to deposition nucleation law provided by Meyers et al. (1992); adapted caption accordingly`

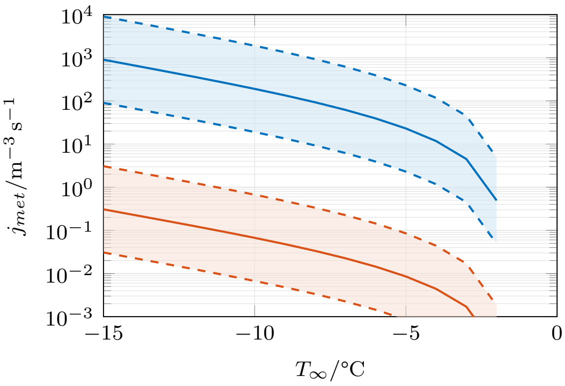

Figure 8: Limiting cases for the nucleation rate j_{met}. The swept-volume limited estimation based on the considerations of Prabhakaran et al. (2020) is shown for $C_{expo} = 10$ (——) with the shaded area depicting the values obtained for $1 < C_{expo} < 100$. The exposure-time limited estimation, which is directly linked to the ice enhancement factor defined in the manuscript, is shown for $\tau_{nucl} = 10$s (——) and the range 1s $< \tau_{nucl} <$ 100s (shaded area).

`Changelog: new figure`

References

Bagchi, P. and Kottam, K.: Effect of Freestream Isotropic Turbulence on Heat Transfer from a Sphere, Physics of Fluids, 20, 073 305, https://doi.org/10.1063/1.2963138, 2008.

Bird, R. B., Stewart, W. E., and Lightfoot, E. N.: Transport Phenomena, second edn., 2002.

Chouippe, A., Krayer, M., Uhlmann, M., Dušek, J., Kiselev, A., and Leisner, T.: Heat and Water Vapor Transfer in the Wake of a Falling Ice Sphere and Its Implication for Secondary Ice Formation in Clouds, New Journal of Physics, 21, 043 043, https://doi.org/10.1088/1367-2630/ab0a94, 2019.

García-García, F. and List, R.: Laboratory Measurements and Parameterizations of Supercooled Water Skin Temperatures and Bulk Properties of Gyrating Hailstones, Journal of the Atmospheric Sciences, 49, 2058–2073, https://doi.org/10.1175/1520-0469(1992)049¡2058:LMAPOS¿2.0.CO;2, 1992.

Johnson, D. A. and Hallett, J.: Freezing and Shattering of Supercooled Water Drops, Quarterly Journal of the Royal Meteorological Society, 94, 468–482, https://doi.org/10.1002/qj.49709440204, 1968.

Lehmann, K., Siebert, H., and Shaw, R. A.: Homogeneous and Inhomogeneous Mixing in Cumulus Clouds: Dependence on Local Turbulence Structure, Journal of the Atmospheric Sciences, 66, 3641–3659, https://doi.org/10.1175/2009JAS3012.1, 2009.

Meyers, M. P., DeMott, P. J., and Cotton, W. R.: New Primary Ice-Nucleation Parameterizations in an Explicit Cloud Model, Journal of Applied Meteorology, 31, 708–721, https://doi.org/10.1175/1520-0450(1992)031¡0708:NPINPI¿2.0.CO;2, 1992.

Prabhakaran, P., Kinney, G., Cantrell, W., Shaw, R. A., and Bodenschatz, E.: High Supersaturation in the Wake of Falling Hydrometeors: Implications for Cloud Invigoration and Ice Nucleation, Geophysical Research Letters, 47, e2020GL088 055, https://doi.org/10.1029/2020GL088055, 2020.

Schiller, L. and Naumann, A.: Über Die Grundlegenden Berechnungen Bei Der Schwerkraftaufbereitung, Z. Ver. Dtsch. Ing, 77, 318–320, 1933.